

University of Groningen

Partial Phase Cohesiveness in Networks of Networks of Kuramoto Oscillators

Qin, Yuzhen; Kawano, Yu; Portoles Marin, Oscar; Cao, Ming

Published in:
IEEE-Transactions on Automatic Control

DOI:
[10.1109/TAC.2021.3062005](https://doi.org/10.1109/TAC.2021.3062005)

IMPORTANT NOTE: You are advised to consult the publisher's version (publisher's PDF) if you wish to cite from it. Please check the document version below.

Document Version
Publisher's PDF, also known as Version of record

Publication date:
2021

[Link to publication in University of Groningen/UMCG research database](#)

Citation for published version (APA):

Qin, Y., Kawano, Y., Portoles Marin, O., & Cao, M. (2021). Partial Phase Cohesiveness in Networks of Networks of Kuramoto Oscillators. *IEEE-Transactions on Automatic Control*, 66(12), 6100-6107. <https://doi.org/10.1109/TAC.2021.3062005>

Copyright

Other than for strictly personal use, it is not permitted to download or to forward/distribute the text or part of it without the consent of the author(s) and/or copyright holder(s), unless the work is under an open content license (like Creative Commons).





The publication may also be distributed here under the terms of Article 25fa of the Dutch Copyright Act, indicated by the "Taverne" license. More information can be found on the University of Groningen website: <https://www.rug.nl/library/open-access/self-archiving-pure/taverne-amendment>.

Take-down policy

If you believe that this document breaches copyright please contact us providing details, and we will remove access to the work immediately and investigate your claim.

Downloaded from the University of Groningen/UMCG research database (Pure): <http://www.rug.nl/research/portal>. For technical reasons the number of authors shown on this cover page is limited to 10 maximum.

Partial Phase Cohesiveness in Networks of Networks of Kuramoto Oscillators

Yuzhen Qin , Member, IEEE, Yu Kawano , Member, IEEE, Oscar Portoles ,
and Ming Cao , Senior Member, IEEE

Abstract—Partial, instead of complete, synchronization has been widely observed in various networks, including, in particular, brain networks. Motivated by data from human brain functional networks, in this article, we analytically show that partial synchronization can be induced by strong regional connections in coupled subnetworks of Kuramoto oscillators. To quantify the required strength of regional connections, we first obtain a critical value for the algebraic connectivity of the corresponding subnetwork using the incremental two-norm. We then introduce the concept of the *generalized complement graph*, and obtain another condition on the node strength by using the incremental ∞ -norm. Under these two conditions, regions of attraction for partial phase cohesiveness are estimated in the forms of the incremental two- and ∞ -norms, respectively. Our result based on the incremental ∞ -norm is the first known criterion that applies to noncomplete graphs. Numerical simulations are performed on a two-level network to illustrate our theoretical results; more importantly, we use real anatomical brain network data to show how our results may contribute to a better understanding of the interplay between anatomical structure and empirical patterns of synchrony.

Index Terms—Kuramoto oscillators, networks of networks, partial synchronization.

I. INTRODUCTION

NEURONAL synchronization across cortical regions of human brain, which has been widely detected through recording and analyzing brain waves, is believed to facilitate communication among neuronal ensembles [1], and only closely correlated oscillating neuronal ensembles can exchange information effectively [2]. In healthy human brain, it is frequently observed that only a part of its cortical regions are synchronized [3], and such a phenomenon is commonly referred to as partial phase cohesiveness or partial synchronization.

Manuscript received February 12, 2020; revised August 26, 2020; accepted February 10, 2021. Date of publication February 24, 2021; date of current version December 3, 2021. This work was supported in part by the European Research Council under Grant ERC-CoG-771687 and in part the Netherlands Organization for Scientific Research under Grant NWO-vidi-14134. Recommended by Associate Editor M. K. Camlibel. (Corresponding author: Yuzhen Qin.)

Yuzhen Qin is with the Department of Mechanical Engineering, University of California, Riverside, CA 92521 USA (e-mail: yuzh.qin@gmail.com).

Yu Kawano is with the Graduate School of Advanced Science and Engineering, Hiroshima University, Higashihiroshima 739-8527, Japan (e-mail: kawano@ieee.org).

Oscar Portoles and Ming Cao are with the Engineering and Technology Institute Groningen and the Department of Artificial Intelligence and Cognitive Engineering, University of Groningen, NL-9747 AG Groningen, The Netherlands (e-mail: o.portoles.marin@rug.nl; ming.cao@ieee.org).

Color versions of one or more figures in this article are available at <https://doi.org/10.1109/TAC.2021.3062005>.

Digital Object Identifier 10.1109/TAC.2021.3062005

In contrast, in pathological brain of a patient, such as an epileptic, excessive synchronization of neural activities takes place across the brain [4]. These observations suggest that healthy brain has powerful regulation mechanisms that are not only able to render synchronization, but also capable of preventing unnecessary synchronization among neuronal ensembles. Partly motivated by these experimental studies, researchers are interested in theoretically studying cluster or partial synchronization [5]–[8] and chimera states [9], even though analytical results are much more difficult to obtain, whereas analytical results for complete synchronization are ample, e.g., [10]–[12].

In our research, our ultimate objective is to identify a possible underlying mechanism of partial phase cohesiveness in the human brain. Employing the Kuramoto model [13], which has been widely used to describe the dynamics of coupled neural ensembles [14], [15], we analytically study how partial phase cohesiveness can occur in a network of coupled oscillators. The human brain can be modeled as a “network of networks” in the sense that adjacent neurons form strongly connected ensembles, which interact weakly with other ensembles [16], [17]. As neural ensembles in a cortical region are adjacent in space, it is thus reasonable to assume that oscillators within a brain region are coupled through an all-to-all network, forming local communities at the lower level; at the higher level, the communities are interconnected by a sparse network facilitated through bundles of neural fibers connecting regions of the brain. Motivated by these facts, we consider in this article the networks describing the interaction between Kuramoto oscillators have this two-level structure.

The main contributions of this article are some new sufficient conditions for partial phase cohesiveness by using Lyapunov functions utilizing the incremental two-norm and ∞ -norm. The incremental two-norm was first proposed in [12] and [18], in which some conditions for locally exponentially stable synchronization were obtained. Later on, it was also employed in the study of noncomplete networks [19], [20]. Inspired by these works, we first employ the incremental two-norm and obtain a sufficient condition for the algebraic connectivity $\lambda_2(L)$ of the considered subnetwork, and then estimate the region of attraction and the ultimate boundedness of phase cohesiveness. This critical value for $\lambda_2(L)$ depends on the natural frequency heterogeneity of the oscillators within the subnetwork and the strength of the connections from its outside to this subnetwork. Since the incremental two-norm depends greatly on the scale, the obtained critical value and the estimated region of attraction are both conservative, especially when there are large numbers of oscillators in the considered subnetwork.

In contrast, the incremental ∞ -norm is scale independent. It is always utilized to prove the existence of phase-locking manifolds and their local stability. Existing conditions are usually expressed implicitly by a combined measure [21], [22], and the regions of attraction are not estimated [7], [23]. To the authors’ best knowledge, the best result on explicit conditions utilizing the incremental ∞ -norm is given in [10], which has only studied uniformly weighted complete networks. To analyze more general networks in terms of the incremental ∞ -norm,

we introduce the concept of the *generalized complement graph* in this article and obtain some novel conditions. Compared to the results obtained by the incremental two-norm: first, the established sufficient condition is less conservative if the dissimilarity of natural frequencies and the strengths of external connections are noticeable; second, more importantly, the region of attraction that we identified is much larger. After simplifying the network structure, our results on partial phase cohesiveness can reduce to some results on complete phase cohesiveness. The reduced results are sharper than the best known result obtained by using incremental two-norm for general connected networks [20, Th. 4.6] (especially in terms of the region of attraction), and are identical to the sharpest one found in [10] for the case of uniformly weighted complete networks. The only drawback of our condition is that each oscillator is required to be connected to a minimum number of other oscillators. Finally, we perform some simulations using the anatomical brain network data obtained in [24]; the simulation results show how our theoretical findings may reveal a possible mechanism that gives rise to various patterns of synchrony detected in empirical data of human brain [25]. Our preliminary work was presented in [26], where only the incremental two-norm was studied. Moreover, we consider a more general intercommunity coupling structure in this article, without requiring that every node in one community is connected to all the nodes in another.

The rest of this article is organized as follows. We introduce the model on the two-level networks and formulate the problem of partial phase cohesiveness in Section II. The first result is obtained by using the incremental two-norm in Section III. Section IV introduces the notion of generalized complement graphs and derives the main result utilizing the incremental ∞ -norm. Some simulations are performed in Section V.

Notations: Let \mathbb{R} and $\mathbb{R}_{\geq 0}$ be the set of real numbers and non-negative real numbers, respectively. For any positive integer n , let $\mathcal{T}_n := \{1, 2, \dots, n\}$, and $\mathbf{1}_n$ be the all-one vector. Denote the unit circle by \mathbb{S}^1 , and a point on it is called a *phase* since the point can be used to indicate the phase angle of an oscillator. For any two phases $\gamma_1, \gamma_2 \in \mathbb{S}^1$, the geodesic distance between them is the minimum of the lengths of the counter-clockwise and clockwise arcs connecting them, which is denoted by $|\gamma_1 - \gamma_2|$. Note that $|\gamma_1 - \gamma_2| \leq \pi$ for any γ_1, γ_2 . Let $\mathbb{T}^n := \mathbb{S}^1 \times \dots \times \mathbb{S}^1$ denote the n -torus. For any $x \in \mathbb{R}$, let $\lfloor x \rfloor$ denote the largest integer that is less than or equal to x , and $\lceil x \rceil$ the smallest integer that is greater than or equal to x . Let $\|\cdot\|_p$ denote the p -norm for both vectors and matrices, where $p \geq 1$ can be infinite.

II. PROBLEM SETUP

We consider a two-level network of Kuramoto oscillators. At the lower level, there are M communities ($M > 1$), each of which consists of N fully connected Kuramoto oscillators ($N > 1$); at the higher level, these communities are interconnected. The dynamics of the oscillators are described by

$$\begin{aligned} \dot{\theta}_i^p &= \omega_i^p + K^p \sum_{n=1}^N \sin(\theta_n^p - \theta_i^p) \\ &+ \sum_{q=1}^M \sum_{n=1}^N a_{i,n}^{p,q} \sin(\theta_n^q - \theta_i^p), \quad p \in \mathcal{T}_M, i \in \mathcal{T}_N \end{aligned} \quad (1)$$

where $\theta_i^p \in \mathbb{S}^1$ and $\omega_i^p \geq 0$ represent the phase and natural frequency of the i th oscillator in the p th community, respectively. Here, the uniform coupling strength¹ of all the edges in the complete graph of the p th community is denoted by $K^p > 0$, which we refer to as the *intracommunity*

coupling strengths. We label the i th oscillator in the p th community by p_i . The coupling strengths $a_{i,n}^{p,q}$, $p \neq q$, which we call the *intercommunity* coupling strengths, satisfy $a_{i,n}^{p,q} > 0$ if there is a connection between the oscillators p_i and q_n , and $a_{i,n}^{p,q} = 0$ otherwise. We define the intercommunity coupling matrices by $A^{p,q} := [a_{i,j}^{p,q}]_{N \times N} \in \mathbb{R}^{N \times N}$, and each satisfies $A^{p,q} = A^{q,p}$. The graph $\mathcal{G} = (\mathcal{V}, \mathcal{E}, W)$ is used to describe this two-level network defined in the following way: $\mathcal{V} = \{p_i\}$ is the set of nodes; $(p_i, q_j) \in \mathcal{E}$ if there is a connection between oscillators p_i and q_j ; W is the weighted adjacency matrix.

The Kuramoto oscillator network model (1) is used in [14] to study synchronization phenomena of human brain. Along this line of research and motivated by brain research data, we focus on studying the widely observed but still not well understood phenomenon for networks of communities of Kuramoto oscillators, the so-called *partial phase cohesiveness*, in which some but not all of the oscillators have close phases. To facilitate the discussion of some properties of interest for a subset of communities in the network, we use $\mathcal{T}_r = \{1, \dots, r\}$, $1 \leq r \leq M$, to denote a set of chosen communities with the aim to investigate how phase cohesiveness can occur among these r communities. We then define the following set to capture the situation when the oscillators in the communities in \mathcal{T}_r reach phase cohesiveness.

Definition 1: Let $\theta \in \mathbb{T}^{MN}$ be a vector composed of the phases of all MN oscillators in all M communities. Then, given \mathcal{T}_r and $\varphi \in [0, \pi]$, define the *partial phase cohesiveness set*

$$\mathcal{S}_\infty(\varphi) := \left\{ \theta \in \mathbb{T}^{MN} : \max_{i,j \in \mathcal{T}_N, k,l \in \mathcal{T}_r} |\theta_i^k - \theta_j^l| \leq \varphi \right\}. \quad (2)$$

Note that φ describes a level of phase cohesiveness since it is the maximum pairwise phase difference of the oscillators in \mathcal{T}_r . The smaller φ is, the more cohesive the phases are. All the phases in \mathcal{T}_r are identical when $\varphi = 0$, which is called *partial phase synchronization*, and this can only happen when all the oscillators have the same natural frequency. In this article, we allow the natural frequencies to be different, and are only interested in the cases where phase differences in \mathcal{T}_r are small enough. We say that partial phase cohesiveness can take place in \mathcal{T}_r if the solution $\theta : \mathbb{R}_{\geq 0} \rightarrow \mathbb{T}^{MN}$ to the system (1) asymptotically converges to this set $\mathcal{S}_\infty(\varphi)$ for some $\varphi \in [0, \pi/2)$. We call the particular case where $\mathcal{T}_r = \mathcal{T}_M$ *complete phase cohesiveness*, which is also called *practical phase synchronization* in [11]. In the rest of this article, we study the partial phase cohesiveness by investigating how a solution $\theta(t)$ can asymptotically converge to the set $\mathcal{S}_\infty(\varphi)$ and also by estimating the value of φ .

Let $\mathcal{G}_r = (\mathcal{V}_r, \mathcal{E}_r, Z)$ denote the subgraph composed of the nodes in the communities contained in \mathcal{T}_r and the edges connecting pairs of them. The weighted adjacency matrix of this subgraph $Z := [z_{ij}]_{Nr \times Nr} \in \mathbb{R}^{Nr \times Nr}$ is then given by

$$Z := \begin{bmatrix} K^1 C & A^{1,2} & \dots & A^{1,r} \\ A^{1,2} & K^2 C & \dots & A^{2,r} \\ \vdots & \vdots & \ddots & \vdots \\ A^{1,r} & A^{2,r} & \dots & K^r C \end{bmatrix} \quad (3)$$

where $C = [c_{ij}]_{N \times N} \in \mathbb{R}^{N \times N}$ is the adjacency matrix of a complete graph with N nodes, where $c_{ij} = 1$ for $i \neq j$, and $c_{ij} = 0$ otherwise. Let $D := \text{diag}(Z \mathbf{1}_{Nr})$, then the Laplacian matrix of the graph \mathcal{G}_r is $L := D - Z$. Let $\lambda_2(L)$ denote the second smallest eigenvalue of L , which is always referred to as the *algebraic connectivity* [27].

Let $\theta^p := [\theta_1^p, \dots, \theta_N^p]^\top$ and $\omega^p := [\omega_1^p, \dots, \omega_N^p]^\top$ for all $p \in \mathcal{T}_M$. As we are only interested in the behavior of the oscillator in \mathcal{G}_r , we

¹We make this assumption of a uniformly weighted complete graph for each community for the convenience of notation. Note that this assumption can be

relaxed by allowing general connected networks without affecting the results in this article.

define $x := [\theta^1, \dots, \theta^r]^\top$ and $\varpi := [\omega^1, \dots, \omega^r]^\top$. For $i \in \mathbb{N}$, we define $\mu(i) := \lceil i/N \rceil$ and $\rho(i) := i - N \cdot \lfloor i/N \rfloor$. Given i , by $\mu(i)$ and $\rho(i)$, one knows that i is the $\rho(i)$ th oscillator in $\mu(i)$ th community. Then, from (1), the dynamics of the oscillators in \mathcal{G}_r can be rewritten as

$$\begin{aligned} \dot{x}_i &= \varpi_i + \sum_{n=1}^{Nr} z_{i,n} \sin(x_n - x_i) \\ &+ \sum_{q=r+1}^M \sum_{n=1}^N a_{\rho(i),n}^{\mu(i),q} \sin(\theta_n^q - x_i) \end{aligned} \quad (4)$$

where $x_i \in \mathbb{S}^1$ and $i \in \mathcal{T}_{Nr}$. The first summation term describes the interactions among the oscillators within the subset of communities \mathcal{T}_r , and the second one represents the interactions from the outside of \mathcal{T}_r to the oscillators in \mathcal{T}_r . In order to study the phase cohesiveness of the oscillators in \mathcal{G}_r , we then look into the dynamics of pairwise phase differences, given by

$$\begin{aligned} \dot{x}_i - \dot{x}_j &= \varpi_i - \varpi_j \\ &+ \sum_{n=1}^{Nr} (z_{i,n} \sin(x_n - x_i) - z_{j,n} \sin(x_n - x_j)) + u_{ij} \\ u_{ij} &:= \sum_{q=r+1}^M \sum_{n=1}^N \left(a_{\rho(i),n}^{\mu(i),q} \sin(\theta_n^q - x_i) \right. \\ &\quad \left. - a_{\rho(j),n}^{\mu(j),q} \sin(\theta_n^q - x_j) \right) \end{aligned} \quad (5)$$

where $i, j \in \mathcal{T}_{Nr}$. Let $\mathbf{u}_r := [u_{ij}]_{i < j} \in \mathbb{R}^{Nr(Nr-1)/2}$. The incremental dynamics (5) play crucial roles in what follows. Similar incremental dynamics are found in [7]. However, we consider a network-of-networks structure, and do not assume that $\varpi_i = \varpi_j$ and $\sum_{q=r+1}^M a_{\rho(i),n}^{\mu(i),q} = \sum_{q=r+1}^M a_{\rho(j),n}^{\mu(j),q}$ for all i, j in \mathcal{T}_{Nr} . In the next two sections, we study partial phase cohesiveness in \mathcal{G}_r with the help of (5) using the incremental two-norm or ∞ -norm (which will be introduced subsequently). To analyze phase cohesiveness, the techniques of ultimate boundedness theorem [28, Th. 4.18] will be employed.

III. INCREMENTAL TWO-NORM

In this section, we introduce the incremental two-norm, and use it as a metric to study partial phase cohesiveness. According to Definition 1, we observe that a partially phase cohesive solution across \mathcal{T}_r should satisfy $|x_i - x_j| \leq \varphi$ for all $i, j \in \mathcal{T}_{Nr}$. A quadratic Lyapunov function has been widely used to study phase cohesiveness even when the graph is not complete [11], [12], [18], [20], which is defined by

$$W(x) := \frac{1}{2} \|B_c^\top x\|_2^2 \quad (6)$$

where $B_c \in \mathbb{R}^{Nr \times (Nr(Nr-1)/2)}$ is the incidence matrix of the complete graph. It is also known as the incremental two-norm metric of phase cohesiveness. For a given $\gamma \in [0, \pi)$, define

$$\mathcal{S}_2(\gamma) := \{\theta \in \mathbb{T}^{MN} : \|B_c^\top x\|_2 \leq \gamma\}. \quad (7)$$

Note that $\mathcal{S}_2(\gamma) \subseteq \mathcal{S}_\infty(\gamma)$ for any given $\gamma \in [0, \pi)$. Different from the existing results that apply to complete cohesiveness taking place among all the oscillators in the networks [11], [12], [18], [20], we have studied partial phase cohesiveness in our previous work [26] using the incremental two-norm metric. Compared to our previous work, we consider more general intercommunity coupling structures as stated in Section II.

Let $\hat{B}_c = |B_c|$ be the elementwise absolute value of the incidence matrix B_c . Let

$$d_i^{\text{ex}} := \sum_{m=r+1}^M \sum_{n=1}^N a_{\rho(i),n}^{\mu(i),m}$$

for all $i \in \mathcal{T}_{Nr}$, and denote

$$D^{\text{ex}} := [d_1^{\text{ex}}, \dots, d_{Nr}^{\text{ex}}]^\top.$$

Now, let us provide our first result on partial phase cohesiveness on incremental two-norm. A similar result can be found in [19, Th. 4.4]. Different from it, we consider a two-level network, i.e., communities of oscillators, and study the partial phase cohesiveness.

Theorem 1: Assume that the algebraic connectivity of \mathcal{G}_r is greater than the critical value specified by

$$\lambda_2(L) > \|B_c^\top \varpi\|_2 + \|\hat{B}_c^\top D^{\text{ex}}\|_2. \quad (8)$$

Then, each of the following equations:

$$\lambda_2(L) \sin(\gamma_s) - \|\hat{B}_c^\top D^{\text{ex}}\|_2 = \|B_c^\top \varpi\|_2$$

$$(\pi/2)\lambda_2(L) \text{sinc}(\gamma_m) - \|\hat{B}_c^\top D^{\text{ex}}\|_2 = \|B_c^\top \varpi\|_2$$

has a unique solution, $\gamma_s \in [0, \pi/2)$ and $\gamma_m \in (\pi/2, \pi]$, respectively, where $\text{sinc}(\eta) = \sin(\eta)/\eta$ for any $\eta \in \mathbb{S}^1$. Furthermore, the following statements hold.

- i) For any $\gamma \in [\gamma_s, \gamma_m]$, $\mathcal{S}_2(\gamma)$ is a positively invariant set of the system (1).
- ii) For any $\gamma \in [\gamma_s, \gamma_m)$, the solution to (1) starting from any $\theta(0) \in \mathcal{S}_2(\gamma)$ converges to the set $\mathcal{S}_2(\gamma_s)$.

△

Proof: Choose $W(x)$ in (6) as a Lyapunov candidate. Similar to the proof of [20, Th. 4.6], we take the time derivative of $W(x)$ along the solution to (1) and obtain

$$\begin{aligned} \dot{W}(x) &\leq x^\top B_c B_c^\top \varpi \\ &\quad - \text{sinc}(\gamma) Nr x^\top B_c \text{diag}(\{z_{ij}\}_{i < j}) B_c^\top x + x^\top B_c \mathbf{u}_r. \end{aligned}$$

From [19, Lemma 7], it holds that

$$x^\top B_c \text{diag}(\{z_{ij}\}_{i < j}) B_c^\top x \geq \lambda_2(L) \|B_c^\top x\|_2^2 / (Nr).$$

From the definition of \mathbf{u}_r , one can evaluate that $\|\mathbf{u}_r\|_2 \leq \|\hat{B}_c^\top D^{\text{ex}}\|_2$. As a consequence, we arrive at

$$\begin{aligned} \dot{W}(x) &\leq x^\top B_c B_c^\top \varpi - \lambda_2(L) \text{sinc}(\gamma) \|B_c^\top x\|_2^2 \\ &\quad + \|B_c^\top x\|_2 \|\hat{B}_c^\top D^{\text{ex}}\|_2. \end{aligned}$$

Following similar steps as those in the proof of [20, Th. 4.6], one can show (i) and (ii) by using the ultimate boundedness theorem [28, Th. 4.18] under condition (8). ■

Suppose there is only one oscillator in each community (i.e., $N = 1$), and it holds that $\mathcal{T}_r = \mathcal{T}_M$, $D^{\text{ex}} = 0$, Theorem 1 reduces to the best-known result on the incremental two-norm in single-level networks [20, Th. 4.6]. One observes that the established result in Theorem 1 is quite restrictive if the number of oscillators is large because we use the incremental two-norm metric. First, the critical value $\lambda_2(L)$ is quite conservative since the right side of (8) depends greatly on the number of oscillator in the network. Second, the region of attraction we have identified in Theorem 1(ii) is quite small. To ensure $\|B_c^\top x(0)\|_2 < \gamma < \pi$, the initial phases are required to be nearly identical. In the next section, we use incremental ∞ -norm, aiming to obtain less conservative results.

IV. INCREMENTAL ∞ -NORM

A. Main Results

In this section, we take the following function as a Lyapunov candidate for partial phase cohesiveness:

$$V(x) = \|B_c^\top x\|_\infty \quad (9)$$

which is also referred to as the incremental ∞ -norm metric. It evaluates the maximum of the pairwise phase differences and, thus, does not depend on the number of oscillators. Then, one notices that $\mathcal{S}_\infty(\varphi)$ in (2) can be rewritten into

$$\mathcal{S}_\infty(\varphi) = \{\theta \in \mathbb{T}^{MN} : V(x) = \|B_c^\top x\|_\infty \leq \varphi\}. \quad (10)$$

To the best of the authors' knowledge, the incremental ∞ -norm has only been used to establish explicit conditions for phase cohesiveness in uniformly weighted complete networks (see [11, Th. 6.6], [10]), although some implicit conditions for general connected networks ensuring local stability of phase-locked solutions are found [21], [22]. Next, we introduce the notion of the *generalized complement* graph, which enables us to apply the incremental ∞ -norm to the analysis of networks that are not necessarily uniformly weighted complete and to obtain some explicit conditions. Given a graph \mathcal{G} , its complement is a graph on the same nodes such that its any two nodes are connected if and only if they are unconnected in \mathcal{G} . The generalized complement is similar to the classical complement, but takes coupling strengths into account.

Definition 2: Consider the weighted undirected graph \mathcal{G} with the weighted adjacency matrix Z , and let K_m be the maximum coupling strength of its edges. Let A_c denote the unweighted adjacency matrix of the complete graph with the same node set as \mathcal{G} . We say $\bar{\mathcal{G}}$ is the *generalized complement* graph of \mathcal{G} if the following two are satisfied: it has the same node set as \mathcal{G} ; the weighted adjacency matrix is given by $\bar{Z} := K_m A_c - Z$.

Let K_m be the maximum element in the matrix (3), and A_c the unweighted adjacency matrix of the complete graph consisting of the same node set as \mathcal{G} . Then, $\bar{Z} := [\bar{z}_{ij}]_{Nr \times Nr} = K_m A_c - Z$ is the weighted adjacency matrix of the generalized complement graph $\bar{\mathcal{G}}$. In order to enable the analysis using the incremental ∞ -norm, we then rewrite (4) into the form taking the difference between the complete graph and the generalized complement graph

$$\begin{aligned} \dot{x}_i &= \varpi_i - K_m \sum_{n=1}^{Nr} \sin(x_i - x_n) + \sum_{n=1}^{Nr} \bar{z}_{i,n} \sin(x_i - x_n) \\ &+ \sum_{q=r+1}^M \sum_{n=1}^N a_{\rho(i),n}^{\mu(i),q} \sin(\theta_n^q - x_i) \end{aligned}$$

where $i \in \mathcal{T}_{Nr}$. Accordingly, the incremental dynamics (5) can be rearranged into

$$\begin{aligned} \dot{x}_i - \dot{x}_j &= \varpi_i - \varpi_j - K_m \sum_{n=1}^{Nr} (\sin(x_i - x_n) - \sin(x_j - x_n)) \\ &+ \sum_{n=1}^{Nr} (\bar{z}_{in} \sin(x_i - x_n) - \bar{z}_{jn} \sin(x_j - x_n)) + u_{ij} \end{aligned} \quad (11)$$

where $i, j \in \mathcal{T}_{Nr}$, and u_{ij} is given by (5).

In the incremental two-norm analysis, the algebraic connectivity plays an important role since it relates to the matrix induced two-norm. When we proceed with the incremental ∞ -norm analysis, the corresponding ideas in terms of the matrix induced ∞ -norm are introduced subsequently. Given a node, its node strength is the sum of the weights

of its associated couplings. Let

$$\bar{D}_m := \|\bar{Z}\|_\infty$$

and refer to it as the *maximum node strength* of the generalized complement graph $\bar{\mathcal{G}}$. Let

$$D_s^{\text{in}} := \min_{i=1, \dots, Nr} \sum_{j=1}^{Nr} z_{ij}$$

which is referred to as the *minimum internal node strength* of \mathcal{G} . Likewise, let the maximum external node strength be

$$D_m^{\text{ex}} := \|D^{\text{ex}}\|_\infty.$$

The following proposition provides a relation between the maximum node strength of $\bar{\mathcal{G}}$ and minimum internal node strength of \mathcal{G} .

Proposition 1: Given the graph \mathcal{G} , its minimum node strength and the maximum node strength of the associated generalized complement graph satisfy $\bar{D}_m = (Nr - 1)K_m - D_s^{\text{in}}$.

Proof: From $\bar{Z} = K_m A_c - Z$, the following holds:

$$\bar{z}_{ij} = \begin{cases} 0, & i = j \\ K_m - z_{ij}, & i \neq j. \end{cases}$$

By taking the summation with respect to j , we have

$$\sum_{j=1}^{Nr} \bar{z}_{ij} = (Nr - 1)K_m - \sum_{j=1}^{Nr} z_{ij}$$

where $z_{ii} = 0$. From the definition of the ∞ -norm of the matrix and the fact that all the elements of \bar{Z} and Z are nonnegative, it follows that

$$\begin{aligned} \bar{D}_m = \|\bar{Z}\|_\infty &= \max_{i=1, \dots, Nr} \left((Nr - 1)K_m - \sum_{j=1}^{Nr} z_{ij} \right) \\ &= (Nr - 1)K_m - \min_{i=1, \dots, Nr} \sum_{j=1}^{Nr} z_{ij} \\ &= (Nr - 1)K_m - D_s^{\text{in}}. \end{aligned}$$

■

Now, we provide our main result in this article.

Theorem 2: Suppose that the minimum internal node strength D_s^{in} is greater than the critical value, i.e.,

$$D_s^{\text{in}} > \frac{\|B_c^\top \varpi\|_\infty + 2D_m^{\text{ex}} + (Nr - 2)K_m}{2}. \quad (12)$$

Then, there exist two solutions, $\varphi_s \in [0, \pi/2)$ and $\varphi_m \in (\pi/2, \pi]$, to the equation $\|B_c^\top \varpi\|_\infty + 2D_m^{\text{ex}} + 2(Nr - 1)K_m - 2D_s^{\text{in}} = NrK_m \sin \varphi$, which are given by

$$\varphi_s = \arcsin \left(\frac{\|B_c^\top \varpi\|_\infty + 2D_m^{\text{ex}} + 2(Nr - 1)K_m - 2D_s^{\text{in}}}{NrK_m} \right) \quad (13)$$

$$\varphi_m = \pi - \varphi_s \quad (14)$$

respectively. Furthermore, the following statements hold.

- For any $\varphi \in [\varphi_s, \varphi_m]$, $\mathcal{S}_\infty(\varphi)$ is a positively invariant set of the system (1).
- For every initial condition $\theta(0) \in \mathbb{T}^{MN}$ such that $\varphi_s < \|B_c^\top x(0)\|_\infty < \varphi_m$, the solution $\theta(t)$ to (1) converges to $\mathcal{S}_\infty(\varphi_s)$. \triangle

Proof: We use (9) as a Lyapunov candidate and compute its upper Dini derivative as a preliminary step. Define $\mathcal{I}'_M(t) := \{i : x_i(t) =$

$\max_{j \in \mathcal{V}_r} x_j(t)$ and $\mathcal{I}'_S(t) := \{i : x_i(t) = \min_{j \in \mathcal{V}_r} x_j(t)\}$. Then, one can rewrite (9) into

$$V(x(t)) = |x_p(t) - x_q(t)| \quad \forall p \in \mathcal{I}'_M(t) \quad \forall q \in \mathcal{I}'_S(t).$$

Next, let $\mathcal{I}_M(t) := \{i : \dot{x}_i(t) = \max_{j \in \mathcal{I}'_M} \dot{x}_j(t)\}$ and $\mathcal{I}_S(t) := \{i : \dot{x}_i(t) = \min_{j \in \mathcal{I}'_S} \dot{x}_j(t)\}$. Then, according to [29, Lemma 2.2], the upper Dini derivative of $V(x(t))$ along the solution to (1) is obtained as

$$\begin{aligned} D^+V(x(t)) &:= \limsup_{\tau \rightarrow 0^+} \frac{V(x(t+\tau)) - V(x(t))}{\tau} \\ &= \dot{x}_m(t) - \dot{x}_s(t) \end{aligned}$$

for all $m \in \mathcal{I}_M(t)$ and $s \in \mathcal{I}_S(t)$. Furthermore, from (11), it follows that

$$\begin{aligned} D^+V(x(t)) &= \varpi_m - \varpi_s - K_m \sum_{n=1}^{Nr} (\sin(x_m - x_n) - \sin(x_s - x_n)) \\ &\quad + \sum_{n=1}^{Nr} (\bar{z}_{mn} \sin(x_m - x_n) - \bar{z}_{sn} \sin(x_s - x_n)) + u_{ms}. \end{aligned}$$

Now, we are ready to prove (i) by showing that $D^+V(x(t)) \leq 0$ when $V(x(t)) = \varphi$. For any $\varphi \in [0, \pi]$, $V(x(t)) = \varphi$ implies that $x_m(t) - x_s(t) = \varphi$. This equation and the trigonometric identity lead to

$$\begin{aligned} \sin(x_m - x_n) - \sin(x_s - x_n) &= 2 \sin(\varphi/2) \cos\left(\frac{x_m - x_n}{2} - \frac{x_n - x_s}{2}\right). \end{aligned}$$

From $x_m(t) - x_s(t) = \varphi$, one notices that

$$-\varphi \leq \frac{x_m - x_n}{2} - \frac{x_n - x_s}{2} \leq \varphi.$$

Consequently, it holds that

$$\cos\left(\frac{x_m - x_n}{2} - \frac{x_n - x_s}{2}\right) \geq \cos\left(\frac{\varphi}{2}\right)$$

and thus

$$\begin{aligned} \sin(x_m - x_n) - \sin(x_s - x_n) &\geq 2 \sin(\varphi/2) \cos(\varphi/2) \\ &= \sin(\varphi) \end{aligned} \quad (15)$$

where the double-angle formula is utilized. On the other hand, recalling the definitions of \bar{D}_m and D_m^{ex} , one knows that

$$\left| \sum_{n=1}^{Nr} (\bar{z}_{mn} \sin(x_m - x_n) - \bar{z}_{sn} \sin(x_s - x_n)) \right| \leq 2\bar{D}_m$$

and $|u_{ms}| \leq 2D_m^{\text{ex}}$. As a consequence, from $\varpi_m - \varpi_s \leq \|B_c^\top \varpi\|_\infty$ and Proposition 1 in addition to (15), we have

$$\begin{aligned} D^+V(x(t)) &\leq \varpi_m - \varpi_s - NrK_m \sin(\varphi) + 2\bar{D}_m + 2D_m^{\text{ex}} \\ &\leq f(\varphi) \end{aligned} \quad (16)$$

where $f(y) := \|B_c^\top \varpi\|_\infty - NrK_m \sin(y) + 2((Nr-1)K_m - D_s^{\text{in}}) + 2D_m^{\text{ex}}$.

Now, we aim to find a subinterval in $[0, \pi]$ such that $f(\varphi) \leq 0$ for any φ in it. If the condition (12) holds, then $f(\pi/2) < 0$ and, thus, there exists such a subinterval around $\varphi = \pi/2$. Moreover, $\sin(y)$ is an increasing and decreasing function in $[0, \pi/2]$ and $[\pi/2, \pi]$, respectively.

Then, there always exist two points $y_1 \in [0, \pi/2]$, $y_2 \in (\pi/2, \pi]$ such that $f(y_1) = f(y_2) = 0$. These two points y_1 and y_2 are nothing but φ_s in (13) and φ_m in (14), respectively. In summary, for any $\varphi \in [\varphi_s, \varphi_m]$, $D^+V(x(t)) \leq 0$ when $V(x(t)) = \varphi$, which implies that $\mathcal{S}_\infty(\varphi)$ is positively invariant.

Next, we prove (ii). Given $x(0)$, it follows from (16) that for any t , there exists $\gamma(t)$ satisfying $\gamma(t) = V(x(t))$ such that

$$\begin{aligned} D^+V(x(t)) &\leq \|B_c^\top \varpi\|_\infty - NrK_m \sin(\gamma(t)) \\ &\quad + 2((Nr-1)K_m - D_s^{\text{in}}) + 2D_m^{\text{ex}}. \end{aligned} \quad (17)$$

Recalling that the initial condition satisfies that $\varphi_s < \|B_c^\top x(0)\|_\infty < \varphi_m$, one knows that $\varphi_s < \gamma(0) < \varphi_m$. Then, the right side of (17) is negative and, thus, the strict inequality $D^+(V(x(0))) < 0$ holds. From $t = 0$ on, $D^+(V(x(0))) < 0$ for all t such that $\varphi_s < \gamma(t) < \varphi_m$, and $D^+(V(x(0))) \leq 0$ if $\gamma(t) = \varphi_s$. One can then conclude that $\theta(t)$ converges to $\mathcal{S}_\infty(\varphi_s)$. ■

The following proposition provides a necessary condition for K_m such that (12) can be satisfied.

Proposition 2: Suppose that D_s^{in} satisfies the condition (12), then K_m satisfies the following inequality:

$$K_m > \frac{\|B_c^\top \varpi\|_\infty + 2D_m^{\text{ex}}}{Nr}. \quad (18)$$

Proof: If the condition (12) is satisfied, we have

$$\|B_c^\top \varpi\|_\infty + 2D_m^{\text{ex}} + (Nr-2)K_m < 2D_s^{\text{in}}.$$

One notices that $D_s^{\text{in}} \leq (Nr-1)K_m$ since there are at most $Nr-1$ edges connecting each node, and the coupling strength of each of them is at most K_m . It then follows that

$$\|B_c^\top \varpi\|_\infty + 2D_m^{\text{ex}} + (Nr-2)K_m < 2(Nr-1)K_m$$

which implies $K_m > (\|B_c^\top \varpi\|_\infty + 2D_m^{\text{ex}})/Nr$.

In the study of synchronization or phase cohesiveness, the network is usually required to be connected. The following proposition shows that the condition (12) implies the connectedness of the graph \mathcal{G}_r since from the condition (12), the minimum internal node strength satisfies $D_s^{\text{in}} > (Nr-2)K_m/2$.

Proposition 3: Consider a graph \mathcal{G} consisting of n nodes. Let K be the maximum coupling strength of its edges. Suppose the minimum node strength of the nodes satisfies $D_s > (n-2)K/2$, then the graph \mathcal{G} is connected.

Proof: We prove this proposition by contradiction. We assume that the graph is not connected, and let i^* and j^* be any two nodes that belongs to two isolated connected components \mathcal{G}_{i^*} and \mathcal{G}_{j^*} , respectively. Let the numbers of nodes that are connected to i^* and j^* be n_{i^*} and n_{j^*} , respectively. The node strength of i^* , denoted by D_{i^*} , satisfies $D_s \leq D_{i^*} \leq n_{i^*}K$. It follows from the assumption $D_s > (n-2)K/2$ that $n_{i^*} > (n-2)/2$, which implies that the number of nodes in \mathcal{G}_{i^*} is strictly greater than $n_{i^*} + 1 = n/2$. Likewise, one can show the number of nodes in \mathcal{G}_{j^*} is strictly greater than $n_{j^*} + 1 = n/2$. Then, the total number of nodes in these two isolated connected components is strictly greater $n_{i^*} + n_{j^*} + 2 = n$, which implies that the number of nodes in the graph \mathcal{G} is greater than n . This is a contradiction and, thus, the network \mathcal{G} is connected. ■

B. Comparisons

We first compare the results in Theorems 1 and 2. It is worth mentioning that the condition in Theorem 2 is less dependent on the number of nodes Nr than that in Theorem 1 in most cases. In sharp contrast to $\|B_c^\top \varpi\|_2$ and $\|\hat{B}_c^\top D^{\text{ex}}\|_2$ in (8), both $\|B_c^\top \varpi\|_\infty$ and D_m^{ex}

in (12) are independent of Nr . Specifically, if we take δ_s and δ_m to be the smallest and largest elements in $|B_c^\top \varpi|$, respectively, it holds that

$$\delta_s \sqrt{Nr(Nr-1)/2} \leq \|B_c^\top \varpi\|_2 \leq \delta_m \sqrt{Nr(Nr-1)/2}.$$

A similar inequality holds for $\|\hat{B}_c^\top D^{\text{ex}}\|_2$. Then, one can observe that $\|B_c^\top \varpi\|_2 + \|\hat{B}_c^\top D^{\text{ex}}\|_2$ in (8) can be much larger than $(Nr-2)K_m/2$ in (12) if Nr is large. More importantly, $\mathcal{S}_\infty(\varphi)$ is much larger than $\mathcal{S}_2(\varphi)$ for the same φ , which implies that the domain of attraction we estimated in Theorem 2 is much larger than that in Theorem 1. Therefore, the convergence to a partially phase cohesive solution is guaranteed by Theorem 2 even if the initial phases are not nearly identical.

On the other hand, the condition (8) can be less conservative than (12), but one would require the natural frequencies to be quite homogeneous, and meanwhile the external connections to be very weak in comparison with K_m . In addition, it can be observed from Proposition 3 that each node in \mathcal{G}_r is required to have more than $(Nr-2)/2$ neighbors from the condition (12). In this sense, the condition (8) is less conservative since it only requires \mathcal{G}_r to be connected.

The following corollary provides a sufficient condition that is independent of the network scale for the partial phase cohesiveness in a dense noncomplete subnetwork \mathcal{G}_r . It is certainly less conservative than its counterpart based on the incremental two-norm.

Corollary 1: Suppose each node in \mathcal{G}_r is connected by at least n_e edges, where $n_e > (Nr-2)/2$, and all the edges have the same weight K . Assume that

$$K > \frac{\|B_c^\top \varpi\|_\infty + 2D_m^{\text{ex}}}{2n_e - (Nr-2)} \quad (19)$$

then the statements (i) and (ii) in Theorem 2 hold. \triangle

The proof follows straightforwardly by letting $D_s^{\text{in}} = n_e K$ and $K_m = K$. Since $2n_e - (Nr-2) \geq 1$, any K satisfying $K > \frac{\|B_c^\top \varpi\|_\infty + 2D_m^{\text{ex}}}{2n_e - (Nr-2)}$ satisfies the condition (19) for any Nr .

Next, we compare our results with some existing ones on cluster synchronization reported in [6]–[8]. Our results share some similarities with them, where strong regional connections are required for partial cohesiveness or synchronization. Different from Menara *et al.* [7] and Tiberi *et al.* [8], we have studied partial phase cohesiveness instead of partial phase synchronization and, thus, the oscillators in the set \mathcal{T}_r are not required to have the same natural frequency. In addition, we have estimated the regions of attraction and ultimate levels of phase cohesiveness, which the existing results [6]–[8] have not shown.

Finally, we compare our results with the previously known works in the literature [10], [20]. Since in the existing results, researchers usually deal with one-level networks, and study the complete phase cohesiveness, we assume, in what follows, that there is only one oscillator in each community in our two-level network, and let the set \mathcal{T}_r in which we want to synchronize the oscillators be the entire community set \mathcal{T}_M . Then, we obtain the following two corollaries.

Corollary 2: Given an undirected graph \mathcal{G} , assume that the following condition is satisfied:

$$D_s^{\text{in}} > \frac{\|B_c^\top \varpi\|_\infty + (M-2)K_m}{2} \quad (20)$$

then the solutions to the equation $\|B_c^\top \varpi\|_\infty + 2D_m^{\text{ex}} + 2(Nr-1)K_m - 2D_s^{\text{in}} = NrK_m \sin \varphi$, $\varphi_s \in [0, \pi/2)$ and $\varphi_m \in (\pi/2, \pi]$ are given by

$$\varphi_s = \arcsin \left(\frac{\|B_c^\top \varpi\|_\infty + 2(M-1)K_m - 2D_s^{\text{in}}}{MK_m} \right)$$

$$\varphi_m = \pi - \varphi_s.$$

Furthermore, the following two statements hold.

- i) For any $\varphi \in [\varphi_s, \varphi_m]$, the set $\mathcal{S}_\infty(\varphi)$ is positively invariant.
- ii) For every initial condition $x(0)$ such that $\varphi_s < |B_c^\top x(0)|_\infty < \varphi_m$, the solution $\theta(t)$ converges to $\mathcal{S}_\infty(\varphi_s)$ asymptotically.

\triangle

This corollary follows from Theorem 2 by letting $N = 1$, $r = M$, and $D_m^{\text{ex}} = 0$. In this case, $K_m = \max_{i,j \in \mathcal{T}_M} a_{ij}$ is the maximum coupling strength in \mathcal{G} . Compared to the best-known result on the incremental two-norm [20, Th. 4.6], the result established in Corollary 2 is often less conservative. The explanation is similar to what we provide when we compare Theorem 2 with Theorem 1. Assuming the network is complete, we obtain the following corollary.

Corollary 3: Suppose the graph \mathcal{G} is complete, and the coupling strength is K/M . Assume that the coupling strength satisfies $K > \|B_c^\top \varpi\|_\infty$. Then, φ_s and φ_m become

$$\varphi_s = \arcsin \left(\frac{\|B_c^\top \varpi\|_\infty}{K} \right), \quad \varphi_m = \pi - \varphi_s.$$

Furthermore, the statements (i) and (ii) in Corollary 2 hold. \triangle

This result is actually identical to the well-known one found in [10, Th. 4.1], which presents phase cohesiveness on complete graphs with arbitrary distributions of natural frequencies.

V. NUMERICAL EXAMPLES

In this section, we provide two examples to show the validity of the obtained results (see Example 1), and also to show their applicability to brain networks (see Example 2). We first introduce the order parameter as a measure of phase cohesiveness [13], which is defined by

$$\nu e^{i\psi} = \frac{1}{n} \sum_{i=1}^n e^{i\theta_j}.$$

The value of ν ranges from 0 to 1. The greater ν is, the higher the node strength of phase cohesiveness becomes. If $\nu = 1$, the phases are completely synchronized; on the other hand, if $\nu = 0$, the phases are evenly spaced on the unit circle \mathbb{S}^1 .

Example 1: We consider a small two-level network consisting of six communities described in Fig. 1(a). Each community consists of five oscillators coupled by a complete graph. We assume that the oscillators between every two adjacent communities are interconnected in a way shown in Fig. 1(b). The intercommunity coupling strengths are given beside the edges in Fig. 1(a). Denote $\omega = [\omega^1, \dots, \omega^6]^\top$, and let $\omega_1 = 0.5$ rad/s and $\omega_i = \omega_1 + 0.1(i-1)$ for all $i = 2, \dots, 30$. Let the intracommunity coupling strengths be $K^2 = K^3 = 2.9$, and $K^1 = K^4 = K^5 = K^6 = 0.01$. One can check that the condition (12) is satisfied for the candidate regions of partial phase cohesiveness in the red rectangular, i.e., $\mathcal{T}_r = \{2, 3\}$. The evolution of the incremental two-norm of the oscillators' phases in \mathcal{T}_r is plotted in Fig. 1(c), from which it can be observed that starting from a value less than φ_m , $\|B_c^\top x(t)\|_\infty$ eventually converges to a value less than φ_s . Then, phase cohesiveness takes place between the communities 2,3. In contrast, it can be seen from Fig. 1(d) that the value of ν remains small, which means that the other communities in the network are always incoherent. These observations validate our obtained results on partial phase cohesiveness in Theorem 2. Moreover, calculating the algebraic connectivity of the subgraph in the red rectangular, we obtain $\lambda_2(L) = 5.6$, which is not sufficient to satisfy the condition (8) in Theorem 1. Consistent with what we have claimed earlier, the results in Theorem 2 can be sharper than those in Theorem 1.

Example 2: In this example, we investigate partial phase cohesiveness in human brain using an anatomical network consisting of 66 cortical regions. The coupling strengths between regions are described

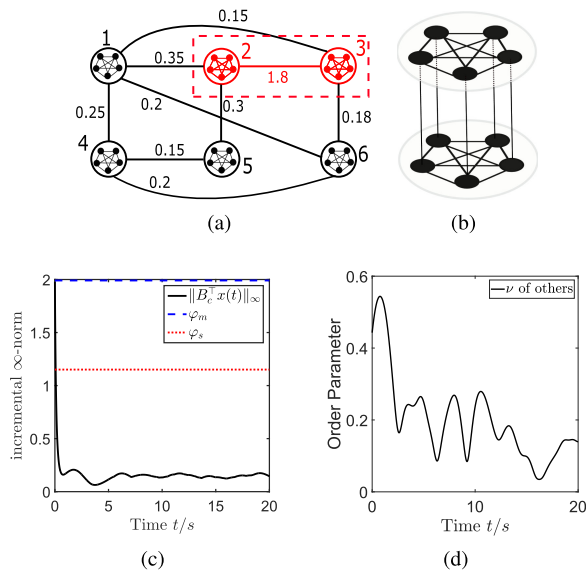


Fig. 1. (a) Network structure considered in Example 1. (b) Interconnection structure: each oscillator in a community is connected to exact one oscillator in another. (c) Trajectory of $\|B_c^p x(t)\|_\infty$, where $x = [\theta_j^p]_{10 \times 1}$, $j \in \mathcal{T}_5$, $p = 2, 3$. (d) Magnitude ν of the order parameter evaluated on other regions (1, 4, 5, and 6).

by a weighted adjacency matrix $A = [a_{ij}]_{66 \times 66}$ whose elements represent axonal fiber densities computed by means of diffusion tensor imaging. This matrix is the average of the normalized anatomical networks obtained from 17 subjects [24]. From our earlier analysis, strong regional connections play an essential role in forming partial phase cohesiveness. We identify some candidate regions by selecting the connections of strengths greater than 20 [visualized by the large size edges in Fig. 2(a)]. In particular, we consider two subsets of the brain regions $\{9, 30, 33\}$ and $\{2, 23\}$ [see the red and blue nodes in Fig. 2(a)], and investigate whether phase cohesiveness can occur among them. Note that the regions $\{9, 30, 33\}$ belong to the auditory network, which have been found to exhibit correlated activity [31].

We use the model in which each of the 66 regions consists of ten oscillators coupled by a complete graph with the coupling strength K^p , $p = 1, \dots, 66$, and any two adjacent regions are connected by ten randomly generated edges. Note that the number of oscillators in each community does not influence our simulation results, and we choose ten just for the convenience of computation. The weights of the ten edges connecting regions i and j are assigned randomly, and sum up to a_{ij} . The natural frequencies of all the oscillators are drawn from a normal distribution $\mathcal{N}(6.5 \text{ Hz}, 4/9 \text{ Hz})$. We chose this frequency range because it has shown transient patterns of synchrony between brain regions during cognitive tasks [25]. However, the selection of a frequency band does not affect our simulation results and only the spread matters. Let the intracommunity coupling strengths $K^p = 8$ for $p = 9, 30, 33$, and $K^p = 0.1$ for all the other p 's. Thus, we have obtained a two-level network from the anatomical brain network. Simulation results in Fig. 2(b) show that the regions, 9, 30, 33, eventually become phase cohesive, although the whole brain remains quite incoherent [see Fig. 2(c), where the mean of ν is approximately 0.15] as expected from Theorem 2. However, the conditions of this theorem are not even satisfied, which implies that they are still conservative. It will be of interest to develop further sharper conditions in the future. On the other hand, Fig. 2(d) shows that without strong intracommunity coupling strengths, phase cohesiveness does not take place between the regions 2 and 23 [the

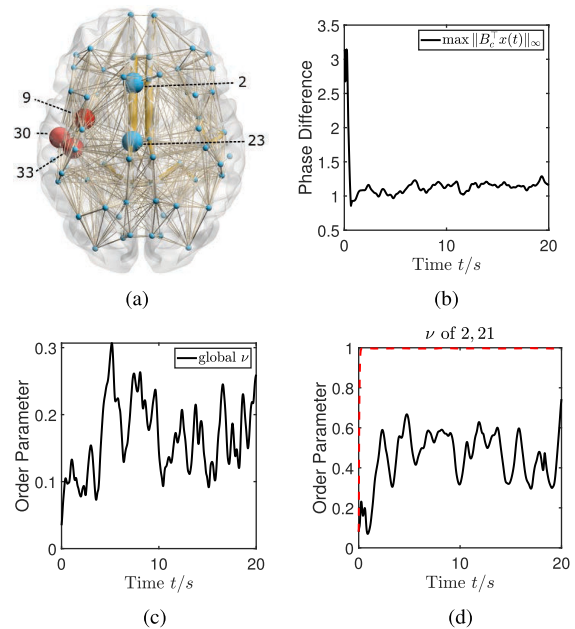


Fig. 2. (a) Anatomical brain network visualized by BrainNet Viewer [30], edges only of weights larger than 0.15 are shown for clarity. (b) Maximum phase difference (absolute value) of the oscillators in 9, 30, 33, where $x = [\theta_j^p]_{30 \times 1}$, $j \in \mathcal{T}_{10}$, $p = 9, 30, 33$. (c) Magnitude ν of the global order parameter. (d) Magnitude ν evaluated on the regions 2 and 23: solid (dashed) line for the absence (presence) of strong intracommunity coupling strengths.

blue large nodes in Fig. 2(a)], although they have a strong interregion connection, $a_{2,23} = 52.8023$. In contrast, letting the intracommunity coupling strengths of regions 2 and 23 be strong ($K^2 = K^{23} = 8$) renders these two regions phase cohesive [see the dashed line in Fig. 2(d)]. This means that intracommunity coupling strengths could play an important role in selecting regions to be synchronized.

From our theoretical results and simulations, we believe that the anatomical properties of the brain network play very important roles in leading to partial synchronization. We conjecture in this article that strong interregional coupling is one of the anatomical properties that allow for synchrony among brain regions. Then, selective synchronization of a subset of those strongly connected regions is achieved by increasing the intracommunity coupling strengths on the target regions, which can give rise to various synchrony patterns. However, this property of anatomical brain networks alone cannot explain all the repertoire of functional connectivity patterns observed in the brain. Other factors, such as the symmetries of the anatomical brain network, can play a role as well [32], [33].

VI. CONCLUSION

We have studied partial phase cohesiveness, instead of complete synchronization, of Kuramoto oscillators coupled by two-level networks in this article. Sufficient conditions in the forms of algebraic connectivity and node strength have been obtained by using the incremental two-norm and ∞ -norm, respectively. The notion of generalized complement graphs that we introduced provides a much better tool than those in the literature to estimate the region of attraction and ultimate level of phase cohesiveness when the network is not uniformly weighted complete. However, the disadvantage of this method is that the number of edges connecting each node has a noticeable lower bound. The simulations

have shown that strong interregional coupling is one of the anatomical properties that could account for partial synchrony observed in the human brain. We are interested in investigating other properties that could render partial synchronization.

REFERENCES

- [1] T. Womelsdorf *et al.*, "Modulation of neuronal interactions through neuronal synchronization," *Science*, vol. 316, no. 5831, pp. 1609–1612, 2007.
- [2] P. Fries, "A mechanism for cognitive dynamics: Neuronal communication through neuronal coherence," *Trends Cogn. Sci.*, vol. 9, no. 10, pp. 474–480, 2005.
- [3] S. Palva and J. M. Palva, "Discovering oscillatory interaction networks with M/EEG: Challenges and breakthroughs," *Trends Cogn. Sci.*, vol. 16, no. 4, pp. 219–230, 2012.
- [4] R. S. Fisher *et al.*, "Epileptic seizures and epilepsy: Definitions proposed by the International League Against Epilepsy (ILAE) and the International Bureau for Epilepsy (IBE)," *Epilepsia*, vol. 46, no. 4, pp. 470–472, 2005.
- [5] L. M. Pecora, F. Sorrentino, A. M. Hagerstrom, T. E. Murphy, and R. Roy, "Cluster synchronization and isolated desynchronization in complex networks with symmetries," *Nature Commun.*, vol. 5, 2014, Art. no. 4079.
- [6] C. Favaretto, A. Cenedese, and F. Pasqualetti, "Cluster synchronization in networks of Kuramoto oscillators," in *Proc. IFAC World Congr.*, Toulouse, France, 2017, pp. 2433–2438.
- [7] T. Menara, G. Baggio, D. Bassett, and F. Pasqualetti, "Stability conditions for cluster synchronization in networks of heterogeneous Kuramoto oscillators," *IEEE Control Netw. Syst.*, vol. 7, no. 1, pp. 302–314, Mar. 2020.
- [8] L. Tiberi, C. Favaretto, M. Innocenti, D. S. Bassett, and F. Pasqualetti, "Synchronization patterns in networks of Kuramoto oscillators: A geometric approach for analysis and control," in *Proc. IEEE Conf. Decis. Control*, Melbourne, FL, Australia, 2017, pp. 7157–7170.
- [9] Y. S. Cho, T. Nishikawa, and A. E. Motter, "Stable chimeras and independently synchronizable clusters," *Phys. Rev. Lett.*, vol. 119, no. 8, 2017, Art. no. 084101.
- [10] F. Dörfler and F. Bullo, "On the critical coupling for Kuramoto oscillators," *SIAM J. Appl. Dyn. Syst.*, vol. 10, no. 3, pp. 1070–1099, 2011.
- [11] F. Dörfler and F. Bullo, "Synchronization in complex networks of phase oscillators: A survey," *Automatica*, vol. 50, no. 6, pp. 1539–1564, 2014.
- [12] A. Jadbabaie, N. Motee, and M. Barahona, "On the stability of the Kuramoto model of coupled nonlinear oscillators," in *Proc. IEEE Amer. Control Conf.*, Boston, MA, USA, 2004, pp. 4296–4301.
- [13] Y. Kuramoto, "Self-entrainment of a population of coupled non-linear oscillators," in *Proc. Int. Symp. Math. Problems Theor. Phys.*, 1975, vol. 39, pp. 420–422.
- [14] H. Schmidt, G. Petkov, M. P. Richardson, and J. R. Terry, "Dynamics on networks: The role of local dynamics and global networks on the emergence of hypersynchronous neural activity," *PLoS Comput. Biol.*, vol. 10, no. 11, 2014, Art. no. e 1003947.
- [15] J. Cabral *et al.*, "Exploring mechanisms of spontaneous functional connectivity in MEG: How delayed network interactions lead to structured amplitude envelopes of band-pass filtered oscillations," *Neuroimage*, vol. 90, pp. 423–435, 2014.
- [16] E. Barreto, B. Hunt, E. Ott, and P. So, "Synchronization in networks of networks: The onset of coherent collective behavior in systems of interacting populations of heterogeneous oscillators," *Phys. Rev. E*, vol. 77, no. 3, 2008, Art. no. 0 36107.
- [17] C. Zhou *et al.*, "Hierarchical organization unveiled by functional connectivity in complex brain networks," *Phys. Rev. Lett.*, vol. 97, no. 23, 2006, Art. no. 238103.
- [18] N. Chopra and M. W. Spong, "On exponential synchronization of Kuramoto oscillators," *IEEE Trans. Autom. Control*, vol. 54, no. 2, pp. 353–357, Feb. 2009.
- [19] F. Dörfler and F. Bullo, "Synchronization and transient stability in power networks and nonuniform Kuramoto oscillators," *SIAM J. Control Optim.*, vol. 50, no. 3, pp. 1616–1642, 2012.
- [20] F. Dörfler and F. Bullo, "Exploring synchronization in complex oscillator networks," in *Proc. IEEE Conf. Decis. Control*, Maui, HI, USA, 2012, pp. 7157–7170.
- [21] F. Dörfler, M. Chertkov, and F. Bullo, "Synchronization in complex oscillator networks and smart grids," *Proc. Nat. Acad. Sci. USA*, vol. 110, no. 6, pp. 2005–2010, 2013.
- [22] S. Jafarpour and F. Bullo, "Synchronization of Kuramoto oscillators via cutset projections," *IEEE Trans. Autom. Control*, vol. 64, no. 7, pp. 2830–2844, Jul. 2019.
- [23] T. Menara, G. Baggio, D. S. Bassett, and F. Pasqualetti, "Exact and approximate stability conditions for cluster synchronization of Kuramoto oscillators," in *Proc. Amer. Control Conf.*, Philadelphia, PA, USA, 2019, pp. 205–210.
- [24] H. Finger *et al.*, "Modeling of large-scale functional brain networks based on structural connectivity from DTI: Comparison with EEG derived phase coupling networks and evaluation of alternative methods along the modeling path," *PLoS Comput. Biol.*, vol. 12, no. 8, 2016, Art. no. e1005025.
- [25] O. Portoles, J. P. Borst, and M. K. van Vugt, "Characterizing synchrony patterns across cognitive task stages of associative recognition memory," *Eur. J. Neurosci.*, vol. 48, no. 8, pp. 2759–2769, 2018.
- [26] Y. Qin, Y. Kawano, and M. Cao, "Partial phase cohesiveness in networks of community Kuramoto oscillators," in *Proc. Euro. Control Conf.*, Limassol, Cyprus, 2018, pp. 2028–2033.
- [27] C. Godsil and G. Royle, *Algebraic Graph Theory*. New York, NY, USA: Springer, 2001.
- [28] H. K. Khalil, *Nonlinear Systems*. Englewood Cliffs, NJ, USA: Prentice-Hall, 2002.
- [29] Z. Lin, B. Francis, and M. Maggiore, "State agreement for continuous-time coupled nonlinear systems," *SIAM J. Control Optim.*, vol. 46, no. 1, pp. 288–307, 2007.
- [30] M. Xia, J. Wang, and Y. He, "BrainNet viewer: A network visualization tool for human brain connectomics," *PLoS One*, vol. 8, no. 7, 2013, Art. no. e 68910.
- [31] L. Heine *et al.*, "Resting state networks and consciousness," *Frontiers Psychol.*, vol. 3, 2012, Art. no. 295.
- [32] V. Nicosia *et al.*, "Remote synchronization reveals network symmetries and functional modules," *Phys. Rev. Lett.*, vol. 110, no. 17, 2013, Art. no. 174102.
- [33] Y. Qin, Y. Kawano, and M. Cao, "Stability of remote synchronization in star networks of Kuramoto oscillators," in *Proc. IEEE Conf. Decis. Control*, Miami Beach, FL, USA, 2018, pp. 5209–5214.